Spinning Black Holes in AGN

Y. Dabrowski
Astrophysics Group, Cavendish Laboratory, Madingley Road, Cambridge CB3 0HE, UK

ABSTRACT

Recent X-ray spectroscopy made with ASCA have shown broad, skewed iron line emission from Seyfert-1 galaxies. The large extent of the red tail allows probing of the innermost regions of the black hole's accretion disc. A model of line emission has been developed and very strong evidence for the presence of a rapidly rotating Kerr black hole has been established in the case of MCG–6-30-15. Issues related to the observed line equivalent width and the position/geometry of the primary source are discussed. Both the continuum and the reflected iron line are computed, in a consistent manner, for a source located on the axis of rotation.

1. Introduction

The iron line in MCG–6-30-15 was found to be both broad and skew from a 4.5 day long observation in 1994 (Tanaka et al. 1995). Much of the skewness is explained by gravitational redshift which gives clear evidence for the effect of strong gravity. In Section 2 we present briefly a simple model of line emission from the accretion disc of a black hole. As explained in more details in Dabrowski et al. (1997), we find that a fit to the line profile observed in MCG–6-30-15 at minimum emission (Iwasawa et al. 1996) gives very strong evidence for a rapidly rotating Kerr black hole. In Section 3 we present a few images of the disc, as a function of the observer's inclination angle and the black hole spin parameter. In Section 4 we investigate the model proposed by Martocchia & Matt (1996) and we predict the observed line equivalent width in the case where the primary hard X-ray source is located on the axis of symmetry, above the accretion disc. Finally, we make a few comments about the forthcoming XMM mission in Section 5.

2. First model, fits to the line profile of MCG–6-30-15

The main parameters to which the line spectra are sensitive are the inclination angle i of the observer from the axis of symmetry, the radial emissivity profile $\epsilon(r)$ of the disc and the angular momentum a/M of the hole. The black hole belongs to the Kerr family and the metric used is in the Boyer-Lindquist form. The accretion disc is assumed to be geometrically thin and axially symmetric around the hole's axis of rotation. The fluorescence emission starts at the radius of marginal stability r_{ms}, up to 15 gravitational radii ($15r_{\rm g} = 15GM/c^2$). In order to concentrate on the influence of i and a/M, the fluorescence emissivity $\epsilon(r)$ is assumed to follow the law described

in Page & Thorne (1974), which closely mimics a power law. However $\epsilon(r)$ vanishes at both r_{ms} and infinity. The observer is located in the asymptotically flat region (in practice at $10^4 r_{\rm g}$). The geometrical setup of the system is described in Figure (1).

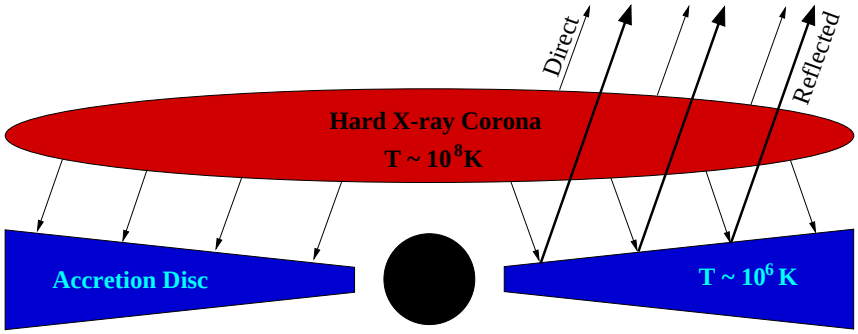

Fig. 1.— The central black hole is surrounded by an accretion disc of 'cold' material. The observed power law spectrum (continuum) originates from the hot, hard X-ray corona assumed to be located above (and below) the disc. The illumination of the disc by hard X-ray photons is responsible for the observed reflected component, including strong fluorescent iron emission lines.

Numerical integration of photon null geodesics are carried out backwards in time, from the observer to the disc, taking into account all the relativistic effects on both trajectory and redshift. The flux at the observer is computed using the phase-space occupation number I_ν/ν^3 which is invariant along the entire photon trajectory. In Dabrowski et al. (1997) we present various predicted spectral lines over a range of a/M and i. We found that the overall width, and in particular the blue cut-off are most sensitive to the inclination angle. For sufficiently high inclination, the line is double peaked, the red and blue peaks being due to the receding and approaching components respectively. In addition, the transverse Doppler and gravitational effects tend to stretch the red wing of the line spectrum. This effect is boosted as the angular momentum increases. Indeed, high values of a/M allow the inner part of the disc to lie closer to the hole, resulting in very strong gravitational effects.

The evidence of strong gravity around a Kerr hole in MCG-6-30-15 has already been discussed by e.g. Iwasawa et al. (1996). Indeed, the study of the variability of the fluorescent iron line profile during the 4.5 day observation has revealed that it broadened still further during a deep minimum in the light curve. The red wing of the line extends further to the low energies while the blue wing disappears. This behaviour can be explained if much of the emission originates from within $6r_{\rm g}$. Since a disc around a non-spinning Schwarzschild black hole does not extend within this region, it is reasonable to conclude that the black hole must be spinning. We have carried out a quantitative χ^2 fit using the disc-line model presented above and obtained joint constraints on both a/M and i (see Dabrowski et al. 1997). The results give relatively good evidence for an inclination angle of $\sim 25^o$ to 30^o and strongly favour an extreme Kerr black hole ($a/M > 0.94$) rather than a Schwarzschild black hole ($a/M = 0$). The inclination $i \sim 30^o$ arises mainly because of the observed cut-off for energies higher than 7 keV, while the observed broad red wing necessitates the high

value of a/M. This result is the first observational evidence of rapidly rotating black holes. From a theoretical point of view, their presence in Active Galactic Nuclei (AGN) was formulated by e.g. K.S. Thorne in 1974. The possibility that AGN harbour a rapidly rotating Kerr black hole is most significant since the hole spin parameter is thought to be the key parameter that would control the formation of relativistic radio jets (e.g. Rees et al.1982).

3. Accretion disc images

As mentioned above, given the inner and outer radii of emission r_{in} and r_{out} and the emissivity law $\epsilon(r)$, disc images depend upon the inclination i and a/M. As an illustration, the images of Figure 2 show the predicted frequency contrast (top three strips) as well as the observed flux (bottom three strips) of the line emission as seen by a distant observer. It is clear, looking at the first column for example, that emission can occur much closer to the central black hole in the case $a/M = 0.998$ than for a Schwarzschild black hole (a/M=0); furthermore, this emission is highly redshifted. Light bending due to strong gravity is clearly visible on these images, particularly at large inclination angles. In the third column the disc is seen edge-on so that one would expect its side only to be visible. What is actually observed at $i = 90^o$ is light from the top of the disc that has been bent at an angle of $\pi/2$ towards the observer. Finally, looking at the middle column for example, one notices that Kerr black holes with $a/M = 0.998$ allow for highly boosted emission from the blue shifted approaching part of the disc.

4. Improved model, problem of equivalent width

For the above model, the line equivalent width is estimated to be $\sim 100 - 200$ eV (see e.g. George & Fabian 1991). However, as discussed in e.g. Nandra et al. (1997) for a sample of 18 Seyfert-1 galaxies, observations reveal equivalent widths of 300 - 600 eV, or even as high as ~ 1 keV in the case of MCG–6-30-15. In order to address this issue, it is necessary to consider in more detail the primary hard X-ray source, responsible for both the continuum and the fluorescence emissions. In particular, as proposed by Martocchia & Matt (1996), the case where the source is located on the rotation axis at a height h above the accretion disc is investigated here (see Figure 3). If the source is close enough to the hole, most of the primary photons are bent towards the disc, enhancing the reflected flux. This effect is negligible for the Schwarzschild case since a large amount of radiation is lost in the event horizon. However, for $a/M \sim 1$ the enhancement should be significantly if the primary source is sufficiently close to the hole ($h < 6r_{\rm g}$). The fluorescence process is taken into account following results given in George & Fabian (1991). Monte Carlo simulations have been carried out for a primary power law energy distribution $N(E) \propto E^{-1.7}$. The seed photons that hit the disc are reprocessed into iron fluorescent photons (6.4 keV) and both the primary and reflected photons that escape to infinity are observed at $i = 30^o$. Consequently, both the continuum and the reflected iron line components can be accounted for in a consistent

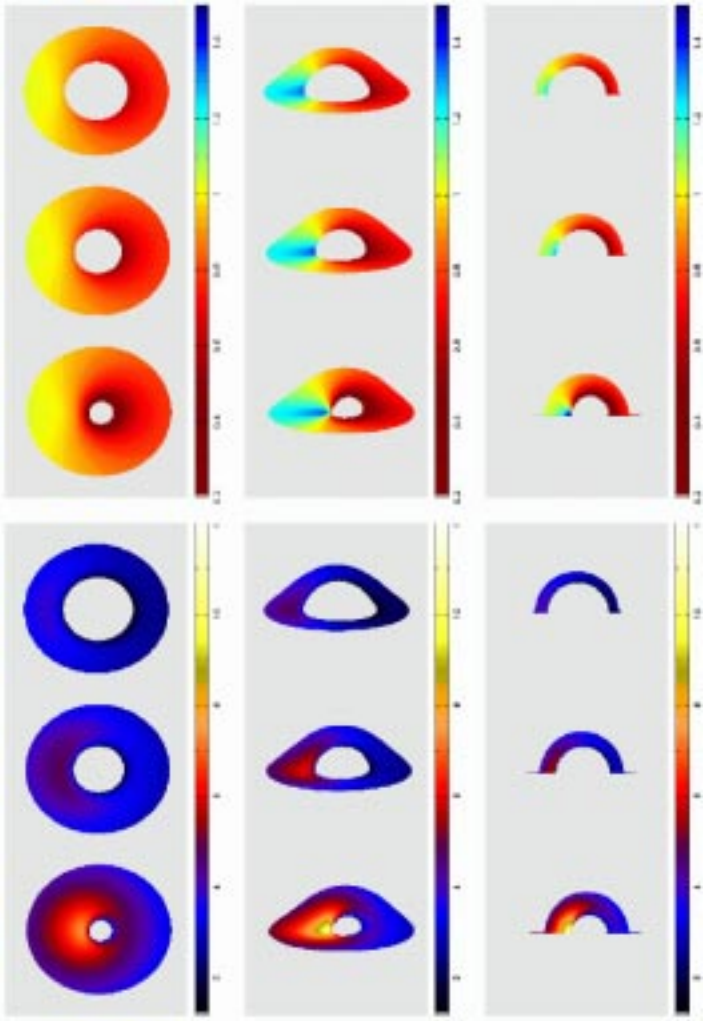

Fig. 2.— Images of accretion discs around Kerr black holes ($r_{in} = r_{ms}$, $r_{out} = 15r_{\rm g}$). The first, second and third columns are for observers with inclination $i = 30^o$, 75^o and 90^o respectively. Each strip is composed of three images which correspond to $a/M = 0$, 0.5 and 0.998, from top to bottom. The colour-scale of the frequency strips (top row) indicates the variation of redshift (ν/ν_0). The colour-scale of the flux strips (bottom row) represents the logarithm of the observed flux.

manner. The fluorescent emission is assumed to start at $r_{in} = r_{ms}$ up to $10^3 r_{\rm g}$ and the observer is located at $10^5 r_{\rm g}$. The predicted equivalent width W_K is found to be $\sim$ 160 eV for a sufficiently distant source ($h > 30r_{\rm g}$), which is in agreement with e.g. George & Fabian (1991) and Matt et al. (1992). As expected, in the case of primary sources located closer to the black hole, a/M plays a fundamental role (see Figure 4). In the case of slowly rotating black holes, no significant equivalent width enhancement is obtained. For rapidly rotating holes, the strong gravitational focusing of light rays combined with emission from the very inner regions contribute to the enhancement of W_K. However, the highest equivalent width obtained is only 300 eV for the extreme case where $a/M = 1$ ($r_{ms} = 1.23r_{\rm g}$) and $h = 2r_{\rm g}$.

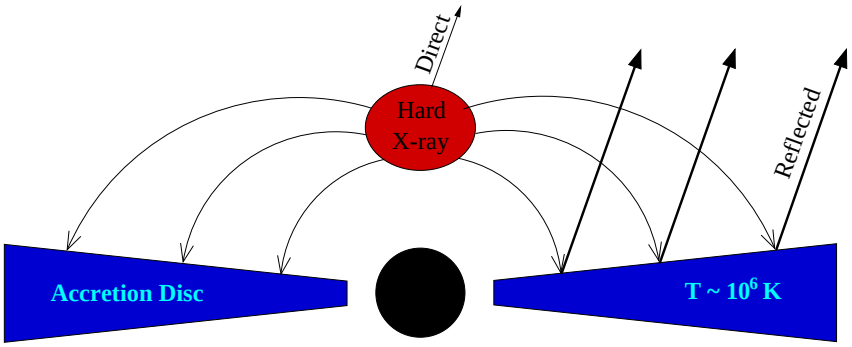

Fig. 3.— New geometry for the primary hard X-ray source. The accretion disc is here illuminated by a source of small extent, placed at height h above the disc, on the axis of symmetry.

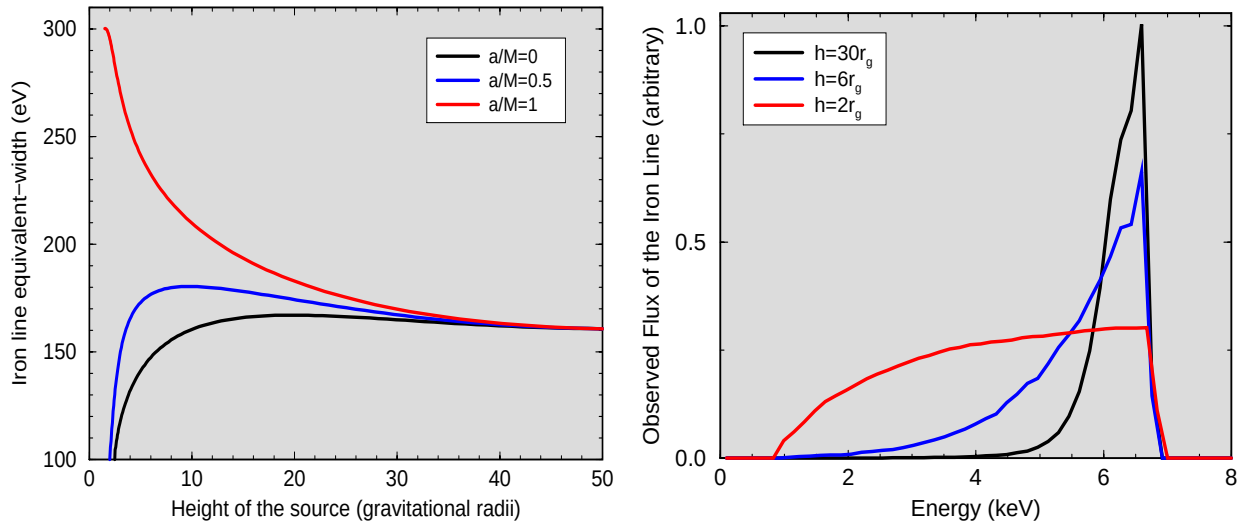

Fig. 4.— **Left**: Measured iron line equivalent width as a function of the height h of the primary source, for $a/M = 0$, 0.5 and 1. Neutral material with cosmic abundances is assumed (George & Fabian, 1991). The Compton reflection continuum is not taken into account. **Right**: Observed iron line profiles for various source height. $a/M = 1$ and $i = 30^o$ are assumed. The flux magnitude is arbitrary, however the area of each line is proportional to its measured equivalent width.

5. The X-ray Multi-mirror Mission

The XMM satellite is several times more sensitive than ASCA, for example. We therefore expect that this new X-ray mission will yield significant returns in understanding AGN central engine and focusing on to properties of supermassive black holes. High resolution spectroscopy will be carried out on many AGN. This will allow more precise study of the iron line profile from samples of AGN larger than considered so far (e.g. Nandra et al. 1997, Bromley et al. 1998). Most of the results concerning black holes characteristics are model dependent and XMM will help in discriminating between different scenarios such as, for example, the occultation model of Weaver

& Yaqoob (1998), or the possibility of iron fluorescence from within the minimum stable orbit r_{ms} proposed by Reynolds & Begelman (1997). Finally recent work by Reynolds et al. (1998), on the temporal response of the iron line to individual activation/flaring of X-ray emitting region, shows how a mission such as XMM will help in constraining the system geometry as well as the black hole mass and angular momentum (see also Fabian et al., this proceedings).

6. Acknowledgements

The work presented here, and particularly in Section 2, is in collaboration with A.C. Fabian, K. Iwasawa, A.N. Lasenby and C.S. Reynolds.

REFERENCES

Bromley, B.C., Miller, W.A., Pariev, V.I. 1998, Nature, 391, 54

Dabrowski, Y., Fabian, A.C., Iwasawa, K., Lasenby, A.N., Reynolds, C.S. 1997, MNRAS, 288, L11

George, I.M., Fabian, A.C. 1991, MNRAS, 249, 352

Iwasawa, K. et al. 1996, MNRAS, 282, 1038

Martocchia, A., Matt, G. 1996, MNRAS, 282, L53

Matt, G., Perola, G.C., Piro, L., Stella, L. 1992, A&A, 257, 63

Nandra, K., George, I.M., Mushotzky, R.F., Turner, T.J., Yaqoob, T. 1997, ApJ, 477, 602

Page, D.N., Thorne, K.S. 1974, ApJ, 499, 191

Rees, M.J., Begelman, M.C., Blandford, R.D., Phinney, E.S. 1982, Nature, 295, 17

Reynolds, C.S., Begelman, M.C. 1997, ApJ, 488, 109

Reynolds, C.S., Young, A.J., Begelman, M.C., Fabian, A.C. 1998, astro-ph/9806327

Tanaka, Y. et al. 1995, Nature, 375, 659

Thorne, K.S. 1974, ApJ, 191, 507

Weaver, K.A., Yaqoob, T. 1998, ApJ, 502, L139